

Pharmacokinetic Optimization of 4-Substituted Methoxybenzoyl-Aryl-Thiazole
(SMART) and 2-Aryl-4-Benzoyl-Imidazole (ABI) for Improving Oral Bioavailability

Chien-Ming Li, Jianjun Chen, Yan Lu, Ramesh Narayanan, Deanna N. Parke, Wei Li,
Sunjoo Ahn, Duane D. Miller, and James T. Dalton

GTx Inc., Memphis, TN, 38163 (C.M.L., R.N., D.N.K., S.A., D.D.M., J.T.D.)

Department of Pharmaceutical Sciences, University of Tennessee Health Science Center,
Memphis, TN 38163 (J. C., Y.L., W.L., D.D.M.)

Running title: DMPK of ABI compounds

Corresponding author:

Name: James T. Dalton PhD

Company: GTx Inc.

Address: 3 N Dunlap Street, Memphis TN, 38163

Telephone: (901)507-8604

Fax: (901)523-9772

E-mail: jdalton@gtxinc.com

Text pages: 27 pages

Tables: 4

Figures: 5

Reference: 26

Words in *Abstract*: 251 words

Words in *Introduction*: 662 words

Words in *Result*: 1531 words

Words in *Discussion*: 677 words

Abbreviations: **SMART-H**, 4-(3, 4, 5-trimethoxybenzoyl)-2-phenyl-thiazole; **ABI**, 2-aryl-4-benzoyl-imidazoles; **MRM**, Multiple reaction monitoring; **PK**, pharmacokinetics; **CAD**, collision-assisted-dissociation; **AUC**, area under the curve; **CYPs**, cytochrome P450s.

Abstract

Microtubules are critical components of the cytoskeleton. Perturbing their function arrests the growth of a broad spectrum of cancer cell lines, making microtubules an excellent and established target for chemotherapy. All of the FDA-approved antitubulin agents bind to paclitaxel- or vinblastine-binding sites in tubulin. Due to the complexity of their structures, it is difficult to structurally modify the vinca alkaloids and taxanes and develop orally bioavailable agents. Antitubulin agents that target the colchicine-binding site in tubulin may provide a better opportunity to be developed for oral use due to their relatively simple structures and physicochemical properties. A potent antitubulin agent, 4-(3, 4, 5-trimethoxybenzoyl)-2-phenyl-thiazole (SMART-H), binding to the colchicine-binding site, was discovered in our laboratory. However, the bioavailability of SMART-H was low due to its poor solubility. Structural modification of SMART-H led to the development of ABI-274 (2-aryl-4-benzoyl-imidazole analog), with improved bioavailability and potency but still considerable first pass metabolism. A chlorine derivative (ABI-286), replacing the methyl site of ABI-274, resulted in 1.5-fold higher metabolic stability *in vitro*, and 1.8-fold lower clearance in rats *in vivo*, indicating that metabolic stability of ABI-274 can be extended by blocking benzylic hydroxylation. Overall, ABI-274 and ABI-286 provided 2.4- and 5.5-fold increases in exposure (AUC) after oral dosing in rats compared to SMART-H. Most importantly, the structural modifications did not compromise potency. ABI-286 exhibited moderate clearance, moderate volume of distribution, and acceptable oral bioavailability. This study provided the first evidence that ABI-286 may be the first member of a new class of orally bioavailable antitubulin agents.

Introduction

Microtubules are critical components of the cytoskeleton and play a pivotal role in spindle formation, cellular shape maintenance, and intracellular transportation (Jordan and Wilson, 2004; Jordan and Kamath, 2007). Due to their critical role in mitosis and cell division, microtubules are regarded as an excellent chemotherapeutic target to treat proliferative oncogenic disorders. Three unique, small-molecule binding sites are known in tubulin and are responsible for the interaction and pharmacologic effect of paclitaxel, vinblastine, and colchicine (Nogales et al., 1998; Gigant et al., 2005). Numerous drugs that target microtubule function and bind to either the paclitaxel or vinca alkaloid binding site have been approved by FDA for the treatment of cancer, including paclitaxel, docetaxel, ixabepilone and vinca alkaloids such as vinblastine, vincristine and vinorelbine. All of these exhibit high potency, but are poorly soluble, require intravenous administration and become less effective in tumors expressing drug efflux transporters. Recently, the search for potent antitubulin agents that are poor P-glycoprotein substrates has intensified (Bollag et al., 1995; Wagner et al., 1999; Sampath et al., 2003; Sampath et al., 2006). However, most of these agents also suffer from poor oral bioavailability due to their high molecular weight and low permeability. Compared to compounds binding the paclitaxel- or vinca alkaloid binding site, antitubulin agents that bind to the colchicine-binding site usually exhibit relatively simple structures, thus providing a better opportunity for structural optimization as orally bioavailable agents. Although several anticancer agents that bind to the colchicine-binding site are being developed, none of them are approved for clinical use (Rustin et al., 2010; Lakhani et al., 2003). A few such agents demonstrate potent tubulin inhibitory properties with a potential for oral use (Tahir

et al., 2003; Hande et al., 2006; Liou et al., 2007). In addition, most of these drugs appear to circumvent P-glycoprotein-mediated drug resistance.

Oral bioavailability is a complex parameter involving many chemical and physiological processes, such as solubility, permeability, and metabolic stability. A potential orally bioavailable drug candidate is expected to have sufficient aqueous solubility to enable it to dissolve and be absorbed in the gastrointestinal tract. Permeability is another key component, as high permeability is necessary for molecules to penetrate across the intestinal lumen into the systemic circulation (Tan et al., 2008). Low clearance is also desired to avoid hepatic first-pass metabolism (Li et al., 2006). When bioavailability is poor, strategies to address these three major factors must be considered in order to identify and overcome the major barriers to oral drug delivery.

Our group recently developed a series of 4-Substituted Methoxybenzoyl-Aryl-Thiazoles (SMART) that bind to the colchicine-binding site and inhibit tubulin polymerization and cancer cell growth at low nanomolar concentrations (Lu et al., 2009). In addition, the SMART compounds circumvented P-glycoprotein-mediated drug resistance and retained potent anticancer activity both *in vitro* and *in vivo* (Li et al., 2011). The SMART compounds demonstrated potency comparable to paclitaxel and exhibited favorable pharmacokinetic properties in rats and dogs when administered intravenously (Li et al., 2010). However, the bioavailability of SMART-H was poor due to its low solubility. In this study, we investigated the low bioavailability of SMART-H and proposed strategies, including enhancement of solubility and metabolic stability, to

improve oral bioavailability. We identified a new series of 2-aryl-4-benzoyl-imidazoles (ABI) with improved aqueous solubility. ABI-182 demonstrated improved bioavailability, as a result of replacing the thiazole with an imidazole ring and enhanced aqueous solubility. One of the most potent molecules in the series, ABI-274, was used as a lead to examine the metabolic stability of the ABI scaffold in human, mouse, rat, and dog liver microsomes. Three major metabolites were identified by LC-MS/MS. ABI-286 was then designed and synthesized to improve metabolic stability based on metabolite identification studies with ABI-274. *In vivo* pharmacokinetic studies were also performed and were in good agreement with *in vitro* metabolic stability. The optimized compound, ABI-286, demonstrated potent *in vitro*, activity and an acceptable bioavailability after oral dosing. These studies shed light on ABI-286's potential as a potent and orally bioavailable tubulin inhibitor.

Materials and Methods

Cell Culture and Cytotoxicity Assay. We examined the antiproliferative activity of the test compounds in a human PC-3 prostate cancer cell lines (ATCC, American Type Culture Collection, Manassas, VA, USA). Cells were cultured in RPMI 1640 (Cellgro Mediatech, Inc., Herndon, VA, USA) supplemented with 10% fetal bovine serum (FBS, Cellgro Mediatech, Manassas, VA) and were maintained at 37°C in a humidified atmosphere containing 5% CO₂. Depending on cell types, 3000 cells were plated into each well of 96-well plates and exposed to different concentrations of the compounds of interest for 96 h. At the end of the treatments, cell viability was measured using the sulforhodamine B (SRB) assay. Percentage of cell survival was plotted against drug concentrations and the IC₅₀ values (concentration that inhibited cell growth by 50% of untreated control) were obtained by nonlinear regression analysis with SigmaPlot (Systat Software Inc., San Jose, CA) using the standard four-parameter logistic curve.

Metabolic incubations. Metabolic stability studies were conducted by incubating 0.5 μM of test compounds in a total reaction volume of 1 mL containing 1 mg/mL microsomal protein in reaction buffer [0.2 M of phosphate buffer solution (pH 7.4), 1.3 mM NADP⁺, 3.3 mM glucose-6-phosphate, and 0.4 U/mL glucose-6-phosphate dehydrogenase] at 37 °C in a shaking water bath. Female rat liver microsomes; pooled human, mouse, and dog liver microsomes were used to examine metabolic stability. ABI-274, at 50 μM concentration, with the above mentioned conditions, was used for metabolite identification studies. The NADPH regenerating system (solution A and B) was obtained from BD Biosciences (Bedford, MA). The total DMSO concentration in the

reaction solution was approximately 0.5% (v/v). Aliquots (100 μ L) from the reaction mixtures used to determine metabolic stability were sampled at 5, 10, 20, 30, 60, and 90 min. Acetonitrile (150 μ L) containing 200 nM of the internal standard was added to quench the reaction and to precipitate the proteins. Samples were then centrifuged at 4,000 g for 15 min at room temperature, and the supernatant was analyzed directly by LC-MS/MS.

Prediction of *in vivo* clearance of ABI-274 and ABI-286 in rat, and human. *In vivo* clearance was predicted utilizing the data obtained from *in vitro* metabolic stability studies (i.e., half-life values in liver microsomes). The intrinsic hepatic clearance ($Cl_{i, in vitro}$) was determined using the equation: $Cl_{i, in vitro} = [0.693 / (t_{1/2, min} \times \text{protein concentration, mg/mL})]$. The intrinsic clearance was then scaled to predict clearance that would occur in the liver *in vivo*. Scaling factors [(mg protein/g liver) \times (g liver/kg body weight)] were 2400, and 1980 for rat, and human, respectively (Li et al., 2010). *In vivo* intrinsic hepatic clearance ($Cl_{i,h}$, ml/min/kg body weight) in liver was estimated by multiplying $Cl_{i, in vitro}$ by the scaling factors. *In vivo* hepatic clearance (Cl_h) was estimated by incorporating estimates of $Cl_{i,h}$, and Q_h into the well-stirred model (venous equation): $Cl_h = [Q_h \times Cl_{i,h} / (Q_h + Cl_{i,h})]$ (Chiba et al., 2009), where Q_h represented hepatic blood flow.

Aqueous solubility. The solubility of drugs was determined by Multiscreen Solubility Filter Plate (Millipore Corporate, Billerica, MA) coupled with LC-MS/MS. Briefly, 198 μ L of phosphate buffered saline (PBS) buffer (pH 7.4) was loaded into 96-well plate, and

2 μ L of 10 mM test compounds (in DMSO) was dispensed and mixed with gentle shaking (200-300 rpm) for 1.5 hours at room temperature (N = 3). The plate was centrifuged at 800g for 10 min, and the filtrate was used to determine its concentration and solubility of test compound by LC-MS/MS as described below.

Pharmacokinetic study. Female Sprague-Dawley rats (N = 3 or 4; 254 ± 4 g) were purchased from Harlan Inc. (Indianapolis, IN). Rat thoracic jugular vein catheters were purchased from Braintree Scientific Inc. (Braintree, MA). On arrival at the animal facility, the animals were acclimated for 3 days in a temperature-controlled room (20–22°C) with a 12-h light/dark cycle before any treatment. All animals were fed prior to dosing, and had access to water ad libitum. SMART-H is a crystalline white solid with purity of 99% as determined by HPLC. All ABI compounds are also solids with >95% purity. Differential Scanning Calorimetry (DSC) studies showed that SMART-H, ABI-182, and ABI-286 are crystalline, while ABI-274 is amorphous. Dosing volumes for intravenous bolus (i.v.) and oral (p.o.) solutions were 2 and 4 mL/kg, respectively. SMART-H was administered i.v. into the thoracic jugular vein at a dose of 2.5 mg/kg (in DMSO/PEG300, 2/8, v/v), whereas ABI-182, ABI-274 and ABI-286 were dosed at 5 mg/kg (in DMSO/PEG300, 1/9, v/v). Catheters were flushed with 1 mL of heparinized saline after i.v. bolus. An equal volume of heparinized saline was injected to replace the removed blood, and blood samples (250 μ L) were collected via the jugular vein catheter at 10, 20, 30 min, and 1, 2, 4, 8, 12, 24 hr. Area under the curve (AUC) values were calculated using the trapezoid rule and extrapolated backward from 10 min to time zero based on the half-life estimated in each animal to minimize the error associated with the

delay between dosing and the first sampling time. SMART-H, ABI-182, and ABI-286 were also given (p.o.) by oral gavage at 10 mg/kg (in Tween80/DMSO/H₂O, 2/1/7, v/v/v) to evaluate their oral bioavailability. ABI-274 (in DMSO/PEG300/H₂O, 2/2/6, v/v/v) was given p.o. at a dose of 10 mg/kg. All blood samples (250 μ L) after oral administration were collected via the jugular vein catheter at 30, 60, 90 min, 120 min, 150 min, 180 min, 210 min, 240 min, and 8, 12, 24 hr. Heparinized syringes and vials were prepared prior to blood collection. Plasma samples were prepared by centrifuging the blood samples at 8,000 g for 5 min. All plasma samples were stored immediately at -80°C until analyzed.

Analytes were extracted from 100 μ L of plasma with 200 μ L of acetonitrile containing 200 nM the internal standard (Figure 1). The samples were thoroughly mixed, centrifuged, and the organic extract was transferred to autosampler for LC-MS/MS analysis. Multiple reaction monitoring (MRM) mode, scanning m/z 356 \rightarrow 188 (SMART-H), m/z 339 \rightarrow 171 (ABI-182), m/z 353 \rightarrow 185 (ABI-274), m/z 373 \rightarrow 205 (ABI-286), and m/z 309 \rightarrow 171 (the internal standard), was used to obtain the most sensitive signals. The pharmacokinetic parameters were determined using non-compartmental analysis (WinNonlin, Pharsight Corporation, Mountain View, CA)

Analytical method. Sample solution (10 μ L) was injected into an Agilent series HPLC system (Agilent 1100 Series Agilent 1100 Chemstation, Agilent Technology Co, Ltd, Santa Clara, CA). All analytes were separated on a narrow-bore C18 column (Alltech Alltima HP, 2.1 \times 100 mm, 3 μ m, Fisher, Fair Lawn, NJ). Two gradient modes were used. For metabolic stability studies, gradient mode was used to achieve the separation of analytes using mixtures of mobile phase A [ACN/H₂O (5%/95%, v/v) containing 0.1%

formic acid] and mobile phase B [ACN/H₂O (95%/5%, v/v) containing 0.1% formic acid] at a flow rate of 300 μ L/min. Mobile phase A was used at 15% from 0 to 1 min followed by a linearly programmed gradient to 100% of mobile phase B within 4 min, 100% of mobile phase B was maintained for 0.5 min before a quick ramp to 15% mobile phase A. Mobile phase A was continued for another 10 min towards the end of analysis. For metabolite identification studies of ABI-274, a slower gradient mode was used to achieve the separation of analytes by using the same flow rate, mobile phase A and B as described. Mobile phase A was used at 5% from 0 to 0.5 min followed by a linearly programmed gradient to 100% of mobile phase B within 9.5 min, 100% of mobile phase B was maintained for 0.5 min before a quick ramp to 5% mobile phase A. Mobile phase A was continued for another 15 min towards the end of analysis.

A triple-quadrupole mass spectrometer, API Qtrap 4000TM (Applied Biosystems/MDS SCIEX, Concord, Ontario, Canada), operating with a TurboIonSpray source was used. The spraying needle voltage was set at 5 kV for positive mode. Curtain gas was set at 10; Gas 1 and gas 2 were set 50. Collision-Assisted-Dissociation (CAD) gas at medium and the source heater probe temperature at 500°C. Data acquisition and quantitative processing were accomplished using AnalystTM software, Ver. 1.4.2 (Applied Biosystems).

Results

4-(3, 4, 5-trimethoxybenzoyl)-2-phenyl-thiazole (SMART-H) exhibits favorable pharmacokinetic properties, but low bioavailability. Previous studies (Li et al., 2010 and 2011) showed that SMART-H (Fig 1) demonstrates potent *in vitro* and *in vivo* antiproliferative activity. SMART-H inhibited the proliferation of a variety of cancer cells *in vitro* with sub-nanomolar IC₅₀ and *in vivo*, in nude mice xenografts, with near 100% tumor growth inhibition. In addition, SMART-H exhibited favorable pharmacokinetic properties in rats and dogs, including low clearance, moderate volume of distribution, and long half-life values. SMART-H was predicted to have low clearance in humans based on the *in vitro-in vivo* correlation model developed in our laboratory. Herein, bioavailability was tested to determine the oral bioavailability of SMART-H. Pharmacokinetic parameters of SMART-H in female rats are summarized in Table 1. The pharmacokinetic parameters for SMART-H in female rats in this study were similar to the pharmacokinetic parameters previously reported for male rats (Li et al., 2010). The oral bioavailability of SMART-H was extremely low, averaging only 3.3 % at a dose of 10 mg/kg. The aqueous solubility of SMART-H was also low ($1.1 \pm 0.1 \mu\text{g/mL}$, Table 2), suggesting that the poor oral bioavailability of SMART-H may due to low solubility.

We considered three major barriers that may contribute to the low oral bioavailability of SMART-H, including aqueous solubility, permeability, and metabolic stability. SMART-H demonstrated low systemic plasma clearance after i.v. dosing, suggesting that hepatic first pass metabolism was not a major factor that would limit oral bioavailability. Permeability studies using Caco-2 cells confirmed that SMART-H has excellent permeability; as the Papp value was $33 \times 10^{-6} \text{ cm/s}$ (A→B) compared to the positive

control, propranolol (Papp 12×10^{-6} cm/s) (data not shown). The aqueous solubility of SMART-H was low (1.1 $\mu\text{g/mL}$). Therefore, SMART-H qualifies as a Biopharmaceutics Classification System (BCS) class II compound, which exhibits low solubility and high permeability. Overall, these data suggested that the low solubility of SMART-H contributed to its limited absorption.

ABI-182 and ABI-274 demonstrates that improved solubility results in improvement of bioavailability. We structurally modified the thiazole moiety of the SMART compounds to an imidazole in an attempt to improve solubility. ABI-182 (Fig 1), an imidazole derivative, exhibited greatly improved solubility ($> 30 \mu\text{g/mL}$) compared to SMART-H, and was selected for pharmacokinetic studies. Figure 2 shows the concentration-time profile of ABI-182 in rats, exhibiting a moderate volume of distribution (1.1 L/kg), but higher systemic plasma clearance (16 mL/min/kg) (Table 1). This structural modification resulted in 4-fold higher systemic exposure (AUC) of ABI-182 compared to SMART-H when administered orally. The oral bioavailability dramatically increased to 24 % (ABI-182) compared to SMART-H (3.3 %), suggesting that aqueous solubility was crucial for absorption (Table 1).

Although ABI-182 demonstrated acceptable bioavailability, it demonstrated 10-fold less *in vitro* potency in PC-3 cancer cell line (Table 2) as compared to SMART-H. ABI-274 was identified as a promising compound in our previous structure activity relationship studies with this class of compounds (Chen et al., 2010). ABI-274 with imidazole ring also exhibited increased solubility and improved systemic exposure and bioavailability (Fig 2 and Table 1) compared to SMART-H.

Benzylic hydroxylation and O-demethylation are the major metabolic pathways for ABI-274. It was important to note that ABI-274's systemic plasma clearance was over 3 times greater than that observed for SMART-H (Table 1), suggesting that its systemic exposure and bio availability were limited due to first-pass hepatic metabolism. We performed *in vitro* metabolism studies to identify the metabolites and labile sites of ABI-274. Table 3 shows the metabolic stability (half-lives) of ABI-274 in human, mouse, rat, and dog liver microsomes. ABI-274 had comparable metabolic stability in human, rat, and dog liver microsomes, but was more quickly metabolized in mouse liver microsomes. As these incubations did not include UDPGA, these data suggest that phase I metabolism plays a significant role in ABI-274 metabolism.

In vitro metabolite identification studies were performed using ABI-274 (50 μ M) and liver microsomes (1 mg/mL) from four species (human, mouse, rat, and dog) to obtain its metabolite profile and to determine metabolically labile sites (i.e., soft spots) in the ABI-274 pharmacophore. LC-MS/MS was used for proposed metabolite identification based on mass shifts compared to the molecular ion $[M+H]^+$ of ABI-274 and retention time shifts to the parent ABI-274. To identify the potential metabolites, the product ion scan for each peak of interest was examined to obtain structural information. Three major metabolites of ABI-274 were identified in human liver microsomes. The product ion spectrum of ABI-274 (Fig 3A) has an abundant product ion m/z 185 (loss of trimethoxy benzene). The metabolite, M1 (m/z 355, mass shifts +2 Da, ketone reduction) (Fig 3B), resulted in the fragment ion m/z 337 (loss of H_2O). The major and the most abundant metabolite in all species, M2 (m/z 369, mass shifts +16 Da, benzylic hydroxylation) (Fig

3C), has an abundant product ion m/z 201 (loss of trimethoxy benzene) and a minor product ion m/z 171 (loss of trimethoxy benzene and CH_2OH). M3 (m/z 339, O-demethylation) (Fig 3D) was present as either the 3- or 4- demethylated metabolite of ABI-274. The mass spectrum could not distinguish between these metabolites since they exhibit identical precursor ion and the same pattern of product ions. Figure 4 shows the multiple-reaction-monitoring (MRM) chromatography of ABI-274 with its three metabolites (M1-M3) after the 1h incubation of ABI-274 (50 μM) in liver microsomes from four different species. Due to higher polarity, all of the metabolites had shorter retention times than ABI-274. M1 (with a retention time of 6.8 min) was only found in human liver microsomes (Fig 4), a result consistent with our previous study (Li et al., 2010). However, it was not the major metabolite in human liver microsomes in this case. M2 (with the retention time at 7.2 or 7.3 min) was the major metabolite in all species. M3 [with the retention time of (7.4 or 7.5) or 7.8 min] presented as positional isomers and could be identified in all species, but with different relative proportions of the 3- or 4-desmethyl metabolite between species. The isomers (M3) were separated based on the gradient chromatographic condition. However, we were unable to determine which of the methoxy groups that was demethylated. The peak eluted at 8.0-8.1 was another hydroxylated metabolite; however, we were unable to determine the hydroxylation site. The overall proposed metabolic pathway for ABI-274 in four species is summarized in Fig 5. Ketone reduction (M1) was apparently unique to human liver microsomes, while benzylic hydroxylation (M2) was the major pathway for all four species. O-demethylation (M3) was also a major pathway in mouse and dog, but not in human and

rat liver microsomes. Overall, these studies suggest that benzylic hydroxylation and O-demethylation were the two predominant mechanisms for ABI-274 metabolism.

Blocking benzylic hydroxylation increased the metabolic stability of ABI-286 in liver microsomes. The two major metabolites of ABI-274 in liver microsomes, M2 (benzylic hydroxylation) and M3 (O-demethylation), indicated the methyl and methoxy groups as the most labile (i.e., soft spots) to metabolism. We thus designed ABI-286 (Fig 1) to incorporate substitutions aimed at improving the metabolic stability of these metabolic soft spots. ABI-286 was designed with a 4-chloro phenyl substituent attached to the imidazole ring to block benzylic hydroxylation. Metabolic stability studies with ABI-286 indicated that blocking benzylic hydroxylation successfully improved the stability in human, mouse, and rat liver microsomes compared to ABI-274 (Table 3). In dog liver microsomes, metabolic stability was slightly increased, but not as much as observed in the other species. The metabolites of ABI-286 were identified and showed that the hydroxylation peak was abolished in all species, confirming that the methyl substituent was the major labile site (data not shown). Most importantly, structural modification in ABI-286 exhibited similar potency, but 12-fold higher solubility compared to SMART-H (Table 2).

Structural changes in ABI-286 improved systemic exposure and oral bioavailability. Rat pharmacokinetic studies were performed to study whether ABI-286 exhibits reduced systemic clearance and increased exposure as suggested by the increase in *in vitro* metabolic stability compared to ABI-274. In Fig 2A, the plasma concentration-time curve

of ABI-286 is shown and compared to ABI-274 by intravenous administration. ABI-286 was eliminated more slowly than ABI-274. The systemic plasma clearance of ABI-286 was 16 mL/min/kg, which was 1.8-fold less than ABI-274 (29 mL/min/kg) (Table 1). ABI-274 and -286 exhibited similar volumes of distributions (1.9 and 2.1 L/kg, respectively). Table 4 summarizes the predicted clearance values based on *in vitro* metabolic stability and scaling methods (described in materials and methods section). The result suggested that *in vivo* clearance correlated well with the data from *in vitro* metabolic stability studies conducted using rat liver microsomes, suggesting that the liver microsome system was an excellent tool to facilitate pharmacokinetic optimization. The predicted *in vivo* clearance values in human are also shown in Table 4. Next, we determined the oral bioavailability of ABI-286. The plasma concentration-time curve of ABI-286 is shown in Fig 2B. The data clearly show that ABI-286 exhibited more than 2-fold increased exposure (AUC) by the oral route as compared to ABI-274. Overall, by p.o. administration, the exposure (AUC) of ABI-286 was 2.4- and 5.5-fold higher than ABI-274 and SMART-H, respectively. The maximal concentration (C_{max}) and bioavailability of ABI-286 were 1088 ng/mL and 32%, respectively (Table 1).

Discussion

The studies and compounds reported in this paper were designed in an attempt to improve the aqueous solubility, metabolic stability and oral bioavailability of a novel series of thiazoles and imidazoles with potent anticancer activity.

Studies with ABI-182 demonstrated a proof-of-concept that enhanced aqueous solubility resulted in improved oral bioavailability (3.3% versus 24 % for SMART-H and ABI-182, respectively). However, ABI-182 exhibited about 11-fold less potency than SMART-H. ABI-274 (a 4-methyl phenyl imidazole derivative) exhibited higher aqueous solubility and greater potency, and was selected for further characterization. Pharmacokinetic studies of ABI-274 in rats revealed that ABI-274 had higher clearance (29 mL/min/kg) than SMART-H (7.7 mL/min/kg). High systemic clearance usually leads to limited oral bioavailability and exposure (AUC) due to first-pass hepatic metabolism. Metabolite identification provided a metabolic perspective to guide synthetic modification and enhance *in vivo* metabolic stability. Interestingly, metabolite identification studies of ABI-274 showed that ketone-reduction was only found in human liver microsomes, a finding consistent with our previous study (Li et al., 2010). However, it was not the major metabolic pathway for ABI-274 as was the case for SMART-H. Benzylic hydroxylation was identified as a major *in vitro* metabolic pathways in all four species (human, mouse, rat and dog), while the extent of O-demethylation varied between species, suggesting that preventing or slowing these processes may improve metabolic stability in all species. Therefore, ABI-286 was designed and synthesized with a 4-chloro substituent replacing the 4-methyl substituent of ABI-274 to block benzylic

hydroxylation and demonstrated improved metabolic stability in liver microsomes of the four species. In addition, ABI-286 did not generate new metabolites in human liver microsomes (data not shown). We also examined the pharmacokinetics of ABI-286 in rats and showed that *in vivo* disposition data correlated well with metabolic stability determined using *in vitro* liver microsomes data. These results confirmed that liver microsome systems provide an accurate and facile method to predict systemic clearance in animals. Similar results were obtained by p.o. administration. The exposure (AUC) of ABI-286 was more than twice that observed for ABI-274, demonstrating that hepatic first-pass metabolism was less for ABI-286 due to reduced benzylic hydroxylation.

Optimization of pharmacokinetic properties is a key to the further improvement of an identified lead compound. An ideal orally bioavailable candidate should exhibit acceptable drug-like properties, including solubility, permeability, and metabolic stability (Vacca et al., 1994; Stegemann et al., 2007). Liver microsomes, which contain several key enzymes such as cytochrome P450s (CYPs), flavin monooxygenases and glucuronosyltransferases required for drug metabolism, are used for *in vitro* metabolic stability studies. Liver microsome systems are also useful tools to perform metabolite identification studies (Watt et al., 2003; Baranczewski et al., 2006). There are several ways to enhance metabolic stability during molecular design (Humphrey and Smith, 1992). In general, metabolic stability may be improved by introduction of a more stable functional group. For example, introduction of a halogen to prevent benzylic or allylic hydroxylation is commonly attempted (Palani et al., 2002). Fortunately, this strategy was successfully applied to the optimization of the SMART and ABI scaffolds. However, the

optimization process sometimes provides unexpected results. Structural modifications at one labile site may result in an increase in the rate of metabolism at another position in the molecule, a phenomenon known as “metabolic switching”. Thus, the lead optimization process for solving a metabolic stability problem is often iterative and time-consuming.

This study showed that the solubility-limited bioavailability (3.3%) of SMART-H could be improved by replacing the thiazole linker with an imidazole and protecting the phenyl ring from oxidation. Importantly, the refined compounds maintained potent anticancer activity. The optimized compound, ABI-286, showed increased metabolic stability and improved oral bioavailability albeit with less *in vitro* potency than ABI-274 and similar to SMART-H. Future studies will examine the influence of other substitutions at the 4-phenyl position to further improve the pharmacokinetic properties of ABI compounds and gain a more comprehensive understanding of their *in vivo* disposition and potential as anticancer agents. Suitable formulations and salt forms of ABI-286 will be also tested in an attempt to further enhance the oral bioavailability of the ABI compounds.

Acknowledgments

We thank Terrence A. Costello, Katie N. Kail and Stacey L. Barnett for providing technical support for animal studies at GTx Inc. We also thank Dr. Tai Ahn for helping on Differential Scanning Calorimetry (DSC) studies.

Authorship Contributions

- Participated in research design: Li CM, Chen, Lu, Narayanan, Li W, Miller, and Dalton.
- Conducted experiments: Li CM, Chen, Lu, Narayanan, and Parke.
- Contributed new reagents or analytic tools: Li CM, Chen, Lu, Li W, Ahn, and Miller.
- Performed data analysis: Li CM, and Dalton.
- Wrote the first draft of the manuscript: Li CM.
- Corresponding author: Dalton.
- Edited and finalized the written manuscript: Dalton.

References

- Baranczewski P, Stanczak A, Kautiainen A, Sandin P and Edlund PO (2006) Introduction to early in vitro identification of metabolites of new chemical entities in drug discovery and development. *Pharmacol Rep* **58**:341-352.
- Bollag DM, McQueney PA, Zhu J, Hensens O, Koupal L, Liesch J, Goetz M, Lazarides E and Woods CM (1995) Epothilones, a new class of microtubule-stabilizing agents with a taxol-like mechanism of action. *Cancer Res* **55**:2325-2333.
- Chen J; Wang Z; Li CM; Lu Y; Vaddady P; Meibohm B; Dalton JT; Miller DD; and Li W (2010) Discovery of novel 2-aryl-4-benzoyl-imidazoles targeting the colchicines binding site in tubulin as potential anticancer agents. *J Med Chem* **53**:7414-27.
- Chiba M, Ishii Y and Sugiyama Y (2009) Prediction of hepatic clearance in human from in vitro data for successful drug development. *Aaps J* **11**:262-276.
- Gigant B, Wang C, Ravelli RB, Roussi F, Steinmetz MO, Curmi PA, Sobel A and Knossow M (2005) Structural basis for the regulation of tubulin by vinblastine. *Nature* **435**:519-522.
- Hande KR, Hagey A, Berlin J, Cai Y, Meek K, Kobayashi H, Lockhart AC, Medina D, Sosman J, Gordon GB and Rothenberg ML (2006) The pharmacokinetics and safety of ABT-751, a novel, orally bioavailable sulfonamide antimetabolic agent: results of a phase 1 study. *Clin Cancer Res* **12**:2834-2840.
- Humphrey MJ and Smith DA (1992) Role of metabolism and pharmacokinetic studies in the discovery of new drugs--present and future perspectives. *Xenobiotica* **22**:743-755.
- Jordan MA and Kamath K (2007) How do microtubule-targeted drugs work? An overview. *Curr Cancer Drug Targets* **7**:730-742.
- Jordan MA and Wilson L (2004) Microtubules as a target for anticancer drugs. *Nat Rev Cancer* **4**:253-265.
- Lakhani NJ, Sarkar MA, Venitz J and Figg WD (2003) 2-Methoxyestradiol, a promising anticancer agent. *Pharmacotherapy* **23**:165-172.
- Li CM, Lu Y, Narayanan R, Miller DD, and Dalton JT (2010) Drug metabolism and pharmacokinetics of 4-Substituted Methoxybenzoyl-Aryl-Thiazole (SMART). *Drug Metabolism Disposition* **38**:2032-2039.
- Li CM, Wang Z, Lu Y, Ahn S, Narayanan R, Kearbey JD, Parke DN, Li W, Miller DD, Dalton JT (2011) Biological activity of 4-Substituted Methoxybenzoyl-Aryl-Thiazole (SMART): An active microtubule inhibitor. *Cancer Res* **71**: 216-224.
- Li HL, Zhang WD, Zhang C, Liu RH, Wang XW, Wang XL, Zhu JB and Chen CL (2006) Bioavailability and pharmacokinetics of four active alkaloids of traditional Chinese medicine Yanhuanglian in rats following intravenous and oral administration. *J Pharm Biomed Anal* **41**:1342-1346.
- Liou JP, Hsu KS, Kuo CC, Chang CY and Chang JY (2007) A novel oral indoline-sulfonamide agent, N-[1-(4-methoxybenzenesulfonyl)-2,3-dihydro-1H-indol-7-yl]-isonicotinamide (J30), exhibits potent activity against human cancer cells in vitro and in vivo through the disruption of microtubule. *J Pharmacol Exp Ther* **323**:398-405.

- Lu Y, Li CM, Wang Z, Ross CR, 2nd, Chen J, Dalton JT, Li W and Miller DD (2009) Discovery of 4-substituted methoxybenzoyl-aryl-thiazole as novel anticancer agents: synthesis, biological evaluation, and structure-activity relationships. *J Med Chem* **52**:1701-1711.
- Nogales E, Wolf SG and Downing KH (1998) Structure of the alpha beta tubulin dimer by electron crystallography. *Nature* **391**:199-203.
- Palani A, Shapiro S, Josien H, Bara T, Clader JW, Greenlee WJ, Cox K, Strizki JM and Baroudy BM (2002) Synthesis, SAR, and biological evaluation of oximino-piperidino-piperidine amides. 1. Orally bioavailable CCR5 receptor antagonists with potent anti-HIV activity. *J Med Chem* **45**:3143-3160.
- Rustin GJ, Shreeves G, Nathan PD, Gaya A, Ganesan TS, Wang D, Boxall J, Poupard L, Chaplin DJ, Stratford MR, Balkissoon J and Zweifel M A (2010) Phase Ib trial of CA4P (combretastatin A-4 phosphate), carboplatin, and paclitaxel in patients with advanced cancer. *Br J Cancer* **102**:1355-1360.
- Sampath D, Discafani CM, Loganzo F, Beyer C, Liu H, Tan X, Musto S, Annable T, Gallagher P, Rios C and Greenberger LM (2003) MAC-321, a novel taxane with greater efficacy than paclitaxel and docetaxel in vitro and in vivo. *Mol Cancer Ther* **2**:873-884.
- Sampath D, Greenberger LM, Beyer C, Hari M, Liu H, Baxter M, Yang S, Rios C and Discafani C (2006) Preclinical pharmacologic evaluation of MST-997, an orally active taxane with superior in vitro and in vivo efficacy in paclitaxel- and docetaxel-resistant tumor models. *Clin Cancer Res* **12**:3459-3469.
- Stegemann S, Leveiller F, Franchi D, de Jong H and Linden H (2007) When poor solubility becomes an issue: from early stage to proof of concept. *Eur J Pharm Sci* **31**:249-261.
- Tahir SK, Nukkala MA, Zielinski Mozny NA, Credo RB, Warner RB, Li Q, Woods KW, Claiborne A, Gwaltney SL, 2nd, Frost DJ, Sham HL, Rosenberg SH and Ng SC (2003) Biological activity of A-289099: an orally active tubulin-binding indolyloxazoline derivative. *Mol Cancer Ther* **2**:227-233.
- Tan W, Chen H, Zhao J, Hu J and Li Y (2008) A study of intestinal absorption of bicyclol in rats: active efflux transport and metabolism as causes of its poor bioavailability. *J Pharm Pharm Sci* **11**:97-105.
- Vacca JP, Dorsey BD, Schleif WA, Levin RB, McDaniel SL, Darke PL, Zugay J, Quintero JC, Blahy OM, Roth E and et al. (1994) L-735,524: an orally bioavailable human immunodeficiency virus type 1 protease inhibitor. *Proc Natl Acad Sci U S A* **91**:4096-4100.
- Wagner MM, Paul DC, Shih C, Jordan MA, Wilson L and Williams DC (1999) In vitro pharmacology of cryptophycin 52 (LY355703) in human tumor cell lines. *Cancer Chemother Pharmacol* **43**:115-125.
- Watt AP, Mortishire-Smith RJ, Gerhard U and Thomas SR (2003) Metabolite identification in drug discovery. *Curr Opin Drug Discov Devel* **6**:57-65.

Footnotes

This work was partially supported by the NIH/NCI [Grant R01CA148706-01A1].

Legends for Figures

Figure 1. Chemical structures of SMART-H, ABI-182, ABI-274, ABT-286, and the internal standard

Figure 2. Pharmacokinetics of ABI-182, -274, and -286. Female Sprague-Dawley rats (N = 3) were dosed with 5 mg/kg by i.v. administration with formulation DMSO/PEG300 (1/9) (A). Sprague-Dawley rats (N = 3) were dosed with 10 mg/kg by p.o. administration of ABI-274 [in DMSO/PEG300/H₂O (2/2/6)]; ABI-182, and -286 [in Tween80/DMSO/H₂O (2/1/7)] (B). Bar, SD.

Figure 3. Proposed metabolites of ABI-274 in human liver microsomes. The parent, ABI-274 (A); M1, ketone reduction (B); M2, benzylic hydroxylation (C); and M3, O-demethylation (D).

Figure 4. Chromatography of ABI-274 and its metabolites. 50 μ M of ABI-274 was incubated with 1 mg/mL microsomal proteins for 1hr at 37°C. Metabolic profile was conducted in human, mouse, rat, and dog liver microsomes. Peak eluted at 8.8min was spiked internal standard.

Figure 5. Proposed metabolites and metabolic pathway of ABI-274 in different species. H, M, R, and D were meant to human, mouse, rat, and dog liver microsomes, and bold means the major metabolites.

Table 1. Pharmacokinetic parameters of SMART-H, ABI-182, ABI-274, and ABI-286 in rats. NR = Not Reported.

	SMART-H		ABI-182		ABI-274		ABI-286	
	IV	PO	IV	PO	IV	PO	IV	PO
Route	IV	PO	IV	PO	IV	PO	IV	PO
N	4	3	3	3	3	3	3	3
Dose	mg/kg		mg/kg		mg/kg		mg/kg	
	2.5	10	5	10	5	10	5	10
CL	mL/min/kg		mL/min/kg		mL/min/kg		mL/min/kg	
	7.7 ± 1.0	NR	16 ± 0.2	NR	29 ± 4	NR	16 ± 3	NR
V _{ss}	L/kg		L/kg		L/kg		L/kg	
	4.9 ± 1.9	NR	1.1 ± 0.2	NR	2.1 ± 0.5	NR	1.9 ± 0.2	NR
t _{1/2}	min		min		min		min	
	925 ± 115	NR	1088 ± 267	NR	703 ± 341	NR	326 ± 190	NR
AUC	min*µg/mL		min*µg/mL		min*µg/mL		min*µg/mL	
	279 ± 53	37 ± 20	306 ± 3	146 ± 12	172 ± 24	87 ± 53	321 ± 77	205 ± 43
C _{max}	ng/mL		ng/mL		ng/mL		ng/mL	
	3816 ± 509	212 ± 65	3877 ± 124	1181 ± 150	2494 ± 272	861 ± 1053	2519 ± 231	1088 ± 403
Apparent T _{max}	min		min		min		min	
	10	60	10	30	10	30	10	60
F	%		%		%		%	
		3.3		24		25		32

Table 2. Cytotoxicity (N=3, mean \pm standard error) in PC-3 cancer cell line and aqueous solubility (N=3, mean \pm standard deviation) of SMART-H, ABI-182, ABI-274, and ABI-286.

^a Previously reported in reference (Lu et al., 2009)

^b Chen et al, 2010.

	IC₅₀ value in PC-3 cell line (nM)	Aqueous solubility ($\mu\text{g}/\text{mL}$)
SMART-H	21 \pm 1^a	1.1 \pm 0.1
ABI-182	288 \pm 30^b	> 30
ABI-274	8.7 \pm 0.4^b	> 30
ABI-286	35 \pm 1^b	12 \pm 2

Table 3. *In vitro* metabolic stability. The percentage of drug remaining was determined by LC-MS/MS. Metabolic stability is presented as half-lives in liver microsomes. Incubations were conducted with 0.5 μ M test compounds and 1 mg/mL liver microsomal proteins in the presence of NADPH at 37°C. (N=3, mean \pm standard deviation)

Liver microsomes	Half-life, min	
	ABI-274	ABI-286
Human	21 \pm 1	44 \pm 6
Mouse	9 \pm 1	23 \pm 2
Rat	30 \pm 2	46 \pm 4
Dog	20 \pm 3	26 \pm 2

Table 4. Prediction of in vivo hepatic clearance of ABI-274 and ABI-286 in rat and human from in vitro metabolic stability. NA = Not Available.

Species Compound	Rat	Rat	Human	Human
	ABI-274	ABI-286	ABI-274	ABI-286
Hepatic blood flow (ml/min/kg)	55	55	21	21
$t_{1/2}$, in liver microsome, min	30	46	21	44
Scaling factor (SF)	2400	2400	1980	1980
SF, (mg protein/g liver * g liver/ kg b.w.)	(54 * 45)	(54 * 45)	(77 * 25.7)	(77 * 25.7)
$Cl_{i, \text{in vitro}}$	0.023	0.015	0.033	0.016
$Cl_{i, h}$	55.44	36.16	65.34	31.19
Cl_h , ml/min/kg (predicted)	28	22	16	13
$Cl_{\text{in vivo}}$	29	16	NA	NA

Figure 1

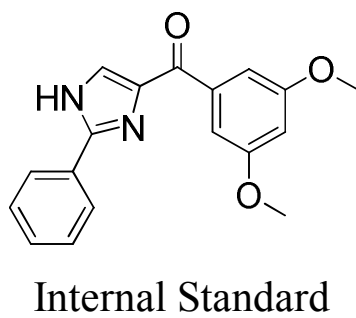
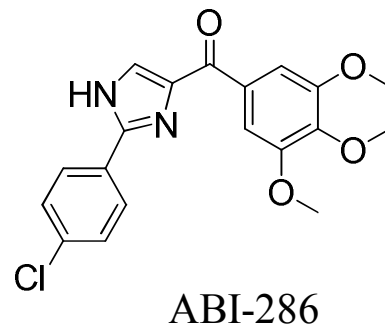
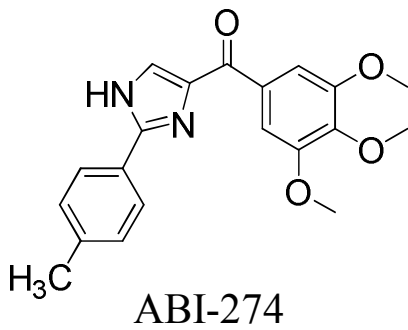
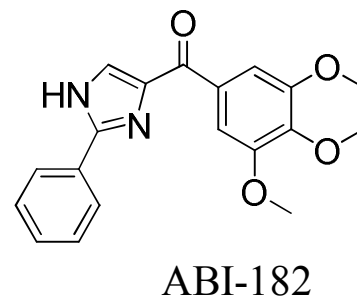
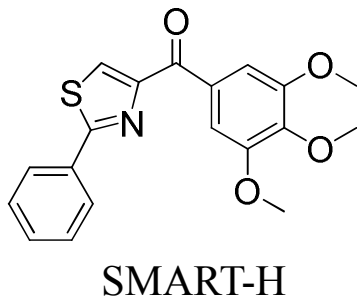


Figure 2

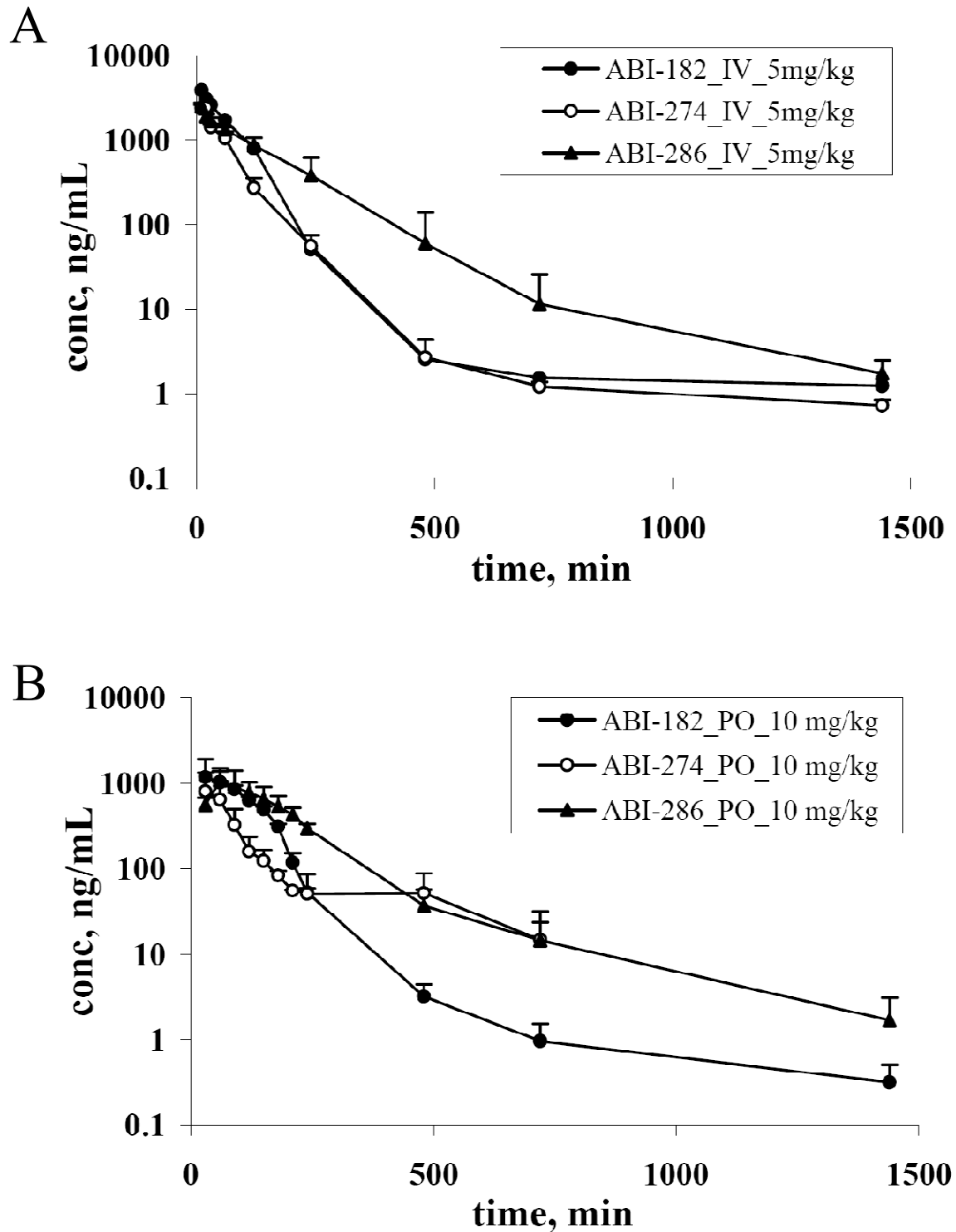


Figure 3

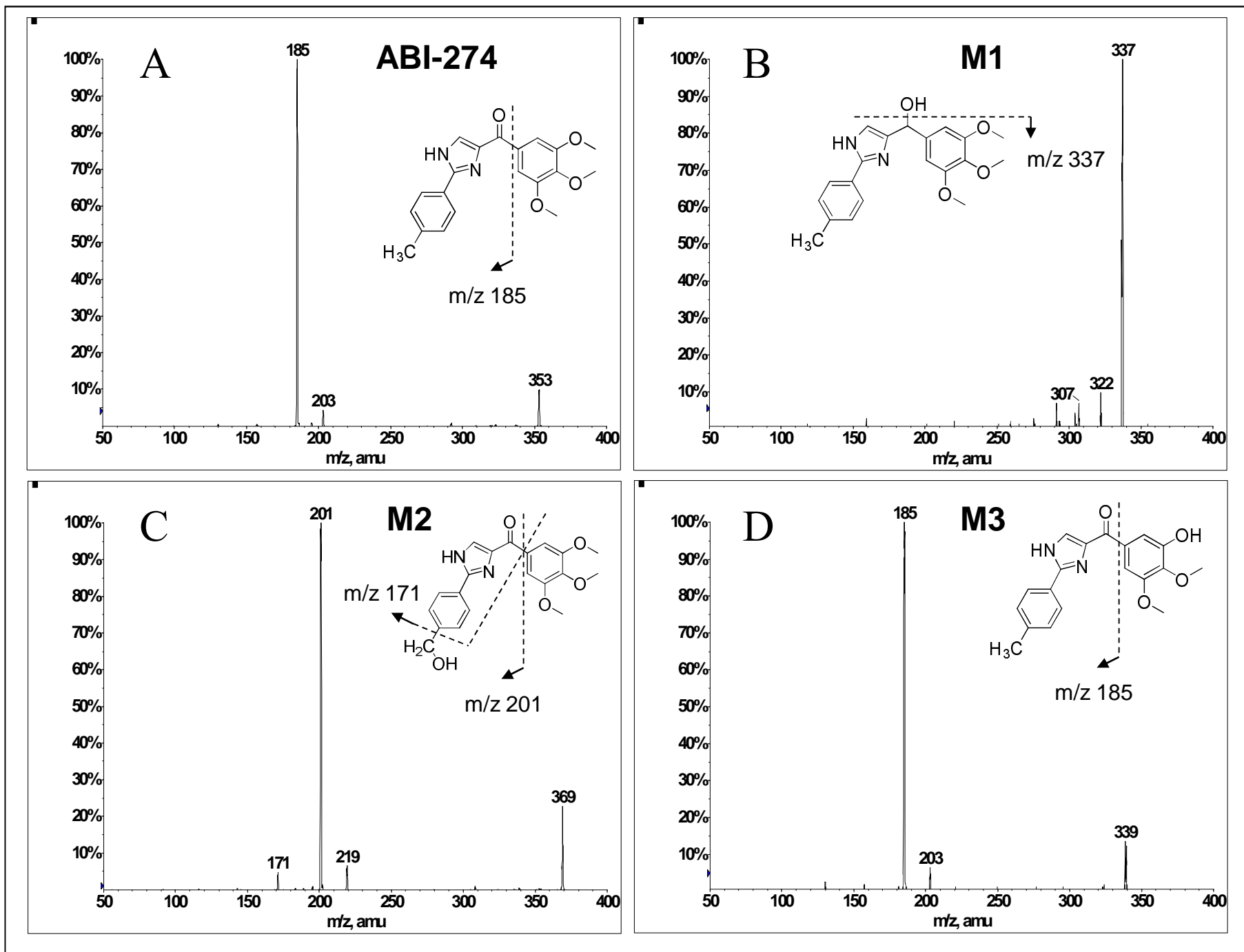


Figure 4

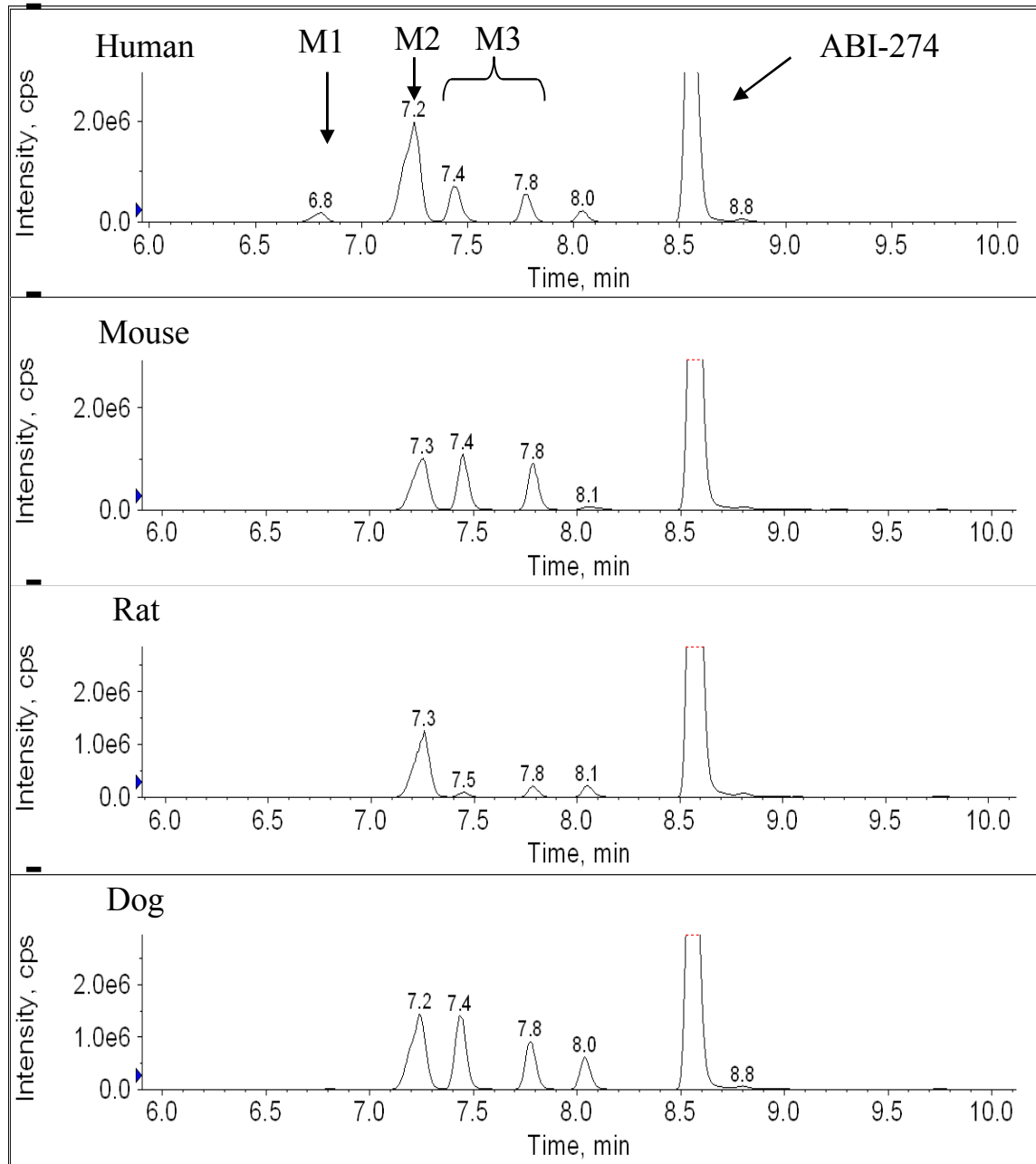


Figure 5

